

1  
2  
3  
4  
5  
6  
7  
8  
9  
10  
11  
12  
13  
14  
15  
16  
17  
18  
19  
20  
21  
22  
23  
24  
25  
26

**Neural representation of current and intended task sets during sequential judgements on human faces**

**Authors:** Paloma Díaz-Gutiérrez<sup>1</sup>, Sam J. Gilbert<sup>2</sup>, Juan E. Arco<sup>1</sup>, Alberto Sobrado<sup>1</sup> & María Ruz<sup>1</sup>

<sup>1</sup>Mind, Brain and Behavior Center, University of Granada

<sup>2</sup>Institute of Cognitive Neuroscience, University College London, UK

**Word count:** 10628

**Contact information:** Department of Experimental Psychology, University of Granada, 18071, Granada, Spain.

Telephone: +34 958 24 06 60. Facsimile number: +34 958 24 62 39

E-mail address: [mrucz@ugr.es](mailto:mrucz@ugr.es) (M. Ruz).

27  
28  
29  
30  
31  
32  
33  
34  
35  
36  
37  
38  
39  
40  
41  
42  
43  
44  
45  
46  
47  
48  
49  
50  
51  
52

## Abstract

Engaging in a demanding activity while holding in mind another task to be performed in the near future requires the maintenance of information about both the currently-active task set and the intended one. However, little is known about how the human brain implements such action plans. While some previous studies have examined the neural representation of current task sets and others have investigated delayed intentions, to date none has examined the representation of current and intended task sets within a single experimental paradigm. In this fMRI study, we examined the neural representation of current and intended task sets, employing sequential classification tasks on human faces. Multivariate decoding analyses showed that current task sets were represented in the orbitofrontal cortex (OFC) and fusiform gyrus (FG), while intended tasks could be decoded from lateral prefrontal cortex (IPFC). Importantly, a ventromedial region in PFC/OFC contained information about both current and delayed tasks, although cross-classification between the two types of information was not possible. These results help delineate the neural representations of current and intended task sets, and highlight the importance of ventromedial PFC/OFC for maintaining task-relevant information regardless of when it is needed.

**Keywords:** delayed intentions, dual-sequential task, PFC, fMRI, MVPA

## 53 1. Introduction

54 The selection and maintenance of relevant information is critical for our ability to pursue  
55 complex and hierarchically organized goals. In cases where we hold delayed intentions  
56 that need to be fulfilled later on (also known as prospective memory; Kliegel, McDaniel,  
57 & Einstein, 2008) or when we perform sequential tasks, it is necessary to represent the  
58 currently-active task and, in addition, the one to be performed later on. It is also important  
59 to switch flexibly from one task set to another (e.g. Monsell, 2003). Some studies have  
60 examined the neural representation of currently-active task sets in frontoparietal areas  
61 (e.g. Waskom, Kumaran, Gordon, Rissman, & Wagner, 2014; Woolgar, Thompson, Bor,  
62 & Duncan, 2011), while others have investigated the representations of delayed intentions  
63 suggesting a key role of medial prefrontal cortex (mPFC) in combination with more  
64 posterior areas (e.g. Gilbert, 2011; Haynes et al., 2007; Momennejad & Haynes, 2013).  
65 However, no previous study has examined the representation of current and intended task  
66 sets within a single experimental paradigm. This combination allows to investigate the  
67 extent to which currently-active and intended future task sets are represented in  
68 overlapping versus distinct brain networks, and also to contrast their activation patterns  
69 directly. Furthermore, previous studies have focused on representations of rather simple  
70 stimuli (i.e. geometric figures, objects, words, etc.; Crittenden, Mitchell, & Duncan, 2015;  
71 Waskom et al., 2014; Woolgar et al., 2011b), so it is not clear how well these findings  
72 generalize to more complex stimuli, such as human faces. In this study, we employed  
73 social categorization dual-sequential judgments on human faces to investigate the  
74 common and differential representation of current and delayed tasks.

75

76 The influence of maintaining an intended task-set on current task performance has  
77 previously been investigated with behavioural methods. These studies highlight how  
78 performance declines with an increment the number of tasks that need to be maintained,

79 showing that the representation of two tasks simultaneously is more demanding compared  
80 to one task only. For instance, Smith (2003) found that participants performed an ongoing  
81 task more slowly when they held in mind a pending intention, compared with performing  
82 the ongoing task alone. This behavioural effect is accompanied by changes in pupil  
83 dilation (Moyes, Sari-Sarraf, & Gilbert, 2019), which also serves as an indicator of task  
84 demands (see van der Wel & van Steenbergen, 2018). Further, dual-task costs have also  
85 been manifested in task switching paradigms, where participants must switch between  
86 two active task-sets (Monsell, 2003; Rogers & Monsell, 1995). Even when the same task  
87 is repeated from the previous trial, responses are slower and less accurate during mixed  
88 blocks (where more than one task is relevant) compared with pure blocks consisting of  
89 just one task (Marí-Beffa, Cooper, & Houghton, 2012).

90

91 Results at the neural level also indicate that the maintenance of two tasks compared with  
92 one alters activity in specific brain regions. Several studies have shown that a set of “task-  
93 positive” regions increase their activation during demanding tasks (also known as the  
94 Multiple Demand network, MD; Duncan, 2010). This network is also sensitive to  
95 cognitive load, increasing its sustained activation as task complexity is raised  
96 (Dumontheil, Thompson, & Duncan, 2011; Palenciano, González-García, Arco, & Ruz,  
97 2019; but see Tschentscher, Mitchell, & Duncan, 2017). Among these areas, the lateral  
98 prefrontal (IPFC) and parietal cortices play a prominent role during dual-task  
99 performance. Both increase their activation during task-switching trials while anterior  
100 PFC shows sustained activation during task-switching blocks (Braver, Reynolds, &  
101 Donaldson, 2003). Similarly, others (Szameitat, Schubert, Müller, & Von Yves Cramon,  
102 2002) have shown involvement of IPFC during dual-task blocks, proportionally to task  
103 difficulty, during simultaneous and interfering task processing. Further, some studies  
104 have employed multivoxel pattern analysis (MVPA) to show how these frontoparietal

105 (FP) regions code current task sets (Palenciano et al., *in press*; Qiao, Zhang, Chen, &  
106 Egner, 2017; Waskom et al., 2014; Woolgar, Hampshire, Thompson, & Duncan, 2011)  
107 and how the representation of task-relevant information in these areas increases with task  
108 demands (Woolgar et al., 2011b).

109

110 Traditionally, the role of FP regions has been opposed to “task-negative” areas, initially  
111 linked to decreased activity during effortful task performance (Fox et al., 2005), although  
112 recent studies suggest that it has a much broader role. This Default Mode Network (DMN)  
113 includes the ventro/dorsomedial PFC, orbitofrontal cortex (OFC), precuneus/posterior  
114 cingulate, inferior parietal lobe (IPL), lateral temporal cortex, and hippocampal formation  
115 (Buckner, Andrews-Hanna, & Schacter, 2008; Raichle, 2015). However, recent studies  
116 have qualified this view, showing that these regions also represent task-relevant  
117 information in different contexts (e.g. Crittenden et al., 2015; González-García et al.,  
118 2017; Palenciano et al., *in press*; Smith, Mitchell, & Duncan, 2018). Moreover, functional  
119 connectivity approaches have shown that the strength of connectivity among task-  
120 negative regions during a working memory task is associated with better performance  
121 (Hampson, Driesen, Skudlarski, Gore, & Constable, 2006). Similarly, Elton and Gao  
122 (2015) observed that the dynamics of connectivity among DMN regions during task  
123 performance were also related to behavioural efficiency. Altogether, the literature  
124 suggests a clear involvement of FP areas in the representation of current task-related  
125 information and highly demanding tasks. Conversely, the role of the DMN is less clear.  
126 Although it shows decreased activation during demanding tasks, its dynamics are also  
127 related to behaviour, and contain task information in different contexts. This suggests that  
128 these regions play a role in the representation of task-relevant knowledge.

129

130 Further, one of the main nodes of the DMN, the medial prefrontal cortex (mPFC) has an  
131 important role in the representation of intended behaviour during both task-free situations  
132 (Haynes et al., 2007) and delays concurrent with an ongoing task (Gilbert, 2011;  
133 Momennejad & Haynes, 2012; Momennejad & Haynes, 2013). This area also plays a role  
134 when holding decisions before they reach consciousness (Soon, Brass, Heinze, & Haynes,  
135 2008). The evidence from studies of delayed intentions has led to suggested dissociations  
136 between the role of lateral and medial PFC (associated with the task-positive and task-  
137 negative networks, respectively). Momennejad & Haynes (2013) directly compared the  
138 representation of future intentions during delays with and without an ongoing task, and  
139 found that while the IPFC had a general role of encoding intentions regardless of whether  
140 there was or not an ongoing task during the delay, the mPFC was involved when the delay  
141 period was occupied by an ongoing task. Alternatively, Gilbert (2011) could not find  
142 encoding of delayed intentions in the IPFC but they did in the mPFC, suggesting that the  
143 former may play a content-free role in remembering delayed intentions while the latter  
144 would represent their specific content. However, these studies vary in the abstraction of  
145 the task rules employed. While Gilbert (2011) aimed to decode specific visual cues and  
146 responses, others focused on the anticipation of abstract task sets, such as arithmetic  
147 operations (addition vs. subtraction; Haynes et al., 2007), or parity vs. magnitude  
148 judgements (Momennejad & Haynes, 2012; Momennejad & Haynes, 2013). This  
149 difference in abstraction could impact the brain region (IPFC vs. mPFC) maintaining  
150 information about future intentions (Momennejad & Haynes, 2013). Further, these studies  
151 also vary in whether the retrieval of the intended task was cued (Gilbert, 2011) or self-  
152 initiated (Momennejad & Haynes, 2012; Momennejad & Haynes, 2013). Therefore,  
153 although these studies have studied the representation of intentions in a variety of  
154 experimental settings, they have not directly addressed how the representation of a future

155 task set may differ from the representation of an ongoing task that is currently being  
156 performed.

157

158 In addition, the studies so far have employed mainly non-social stimuli. In this context it  
159 is worth noting that the DMN has also been related to processes relevant in the social  
160 domain (Buckner & Carroll, 2007; Mars et al., 2012; Spreng, Mar, & Kim, 2008). For  
161 instance, engagement of the DMN during rest is related to better memory for social  
162 information (Meyer, Davachi, Ochsner, & Lieberman, 2018). Facial stimuli are an  
163 important source of social knowledge, which is represented in a set of regions including  
164 the fusiform gyri (FG; Haxby, Hoffman, & Gobbini, 2000; Kanwisher & Yovel, 2006).  
165 This FG also shows different neural patterns distinguishing social categories (Kaul,  
166 Ratner, & Van Bavel, 2014; Stolier & Freeman, 2017). Similarly, the representational  
167 structure of social categories is altered by personal stereotypes both in the FG and in  
168 higher-level areas such as the OFC (Stolier & Freeman, 2016), which is also linked to the  
169 representation of social categories such as gender, race, or social status (Gilbert,  
170 Swencionis, & Amodio, 2012; Kaul, Rees, & Ishai, 2011; Koski, Collins, Olson, &  
171 Hospital, 2017) and the integration of contextual knowledge during face categorization  
172 (Freeman et al., 2015). Likewise, during predictive face perception, the FG coactivates  
173 with and receives top-down influences from dorsal and ventral mPFC (e.g. Summerfield  
174 et al., 2006), which in turn have also been implicated on judgements about faces  
175 (Mitchell, Macrae, & Banaji, 2006; Singer, Kiebel, Winston, Dolan, & Frith, 2004).  
176 Therefore, given the special properties and influence of social information gathered from  
177 faces, understanding how task-relevant current and delayed information may be  
178 represented when it pertains to social information is important to extend and complement  
179 previous findings.

180

181 In the current fMRI study, we employed a dual-sequential categorization task, where  
182 participants had to discriminate between features of three dimensions of facial stimuli and  
183 had to maintain for a period of time both the initial ongoing task and an intended one. In  
184 particular, we studied how demands (one vs. two sequential tasks) influence performance,  
185 and hypothesized that high demand would be associated with worse performance  
186 alongside with activation in frontoparietal regions, especially the IPFC. To examine the  
187 brain regions containing fine-grained information about both current and intended tasks  
188 we employed MVPA. Unlike traditional univariate methods, where the mean activation  
189 in a set of voxels is compared between conditions, MVPA focuses on the spatial  
190 distribution of activations. Here, a classifier is trained to distinguish response patterns  
191 associated with different experimental conditions (i.e. stimuli categories, cognitive states,  
192 etc.) in a certain brain region. If the trained classifier is able to predict the patterns of  
193 independent data, there is indication that the brain area under study represents specific  
194 information about those conditions. Thus, MVPA allows to examine finer-grained  
195 differences in how information is represented in the brain (for reviews see Haxby,  
196 Connolly, & Guntupalli, 2014; Haynes, 2015). In this work, we aimed to study how an  
197 intended task set might be represented differently from a currently-active ongoing task.  
198 For that reason, we focused on the initial pre-switch period, when the current task is being  
199 performed before switching to the intended task. Specifically, we performed separate  
200 analyses to decode: 1) the task currently being performed, regardless of the intended  
201 future task; 2) the task intended for the future, regardless of the current task (henceforth:  
202 “initial task” and “intended task”, respectively). Given the extensive literature associating  
203 FP areas to the representation of task-relevant information (Qiao et al., 2017; Waskom et  
204 al., 2014; Woolgar et al., 2011a, 2011b), we expected to decode the initial relevant task  
205 in MD regions and the intended one in “task-negative” regions, especially the mPFC, in

206 line with previous studies showing its role in prospective memory (Gilbert, 2011; Haynes  
207 et al., 2007; Momennejad & Haynes, 2012; Momennejad & Haynes, 2013) .

208

## 209 **2. Methods**

### 210 **2.1. Participants**

211 Thirty-two volunteers were recruited through adverts addressed to undergraduates and  
212 postgraduate students of the University of Granada (range: 18-28,  $M = 22.5$ ,  $SD = 2.84$ ,  
213 12 men). All of them were Caucasian, right-handed with normal or corrected-to-normal  
214 vision and received economic remuneration (20-25 Euros, according to performance) in  
215 exchange for their participation. Participants signed a consent form approved by the  
216 Ethics Committee for Human Research of the University of Granada.

217

### 218 **2.2. Apparatus and stimuli**

219 We employed 24 face photographs (12 identities, 6 females, 6 black; 3 different identities  
220 per sex and race) displaying happy or angry emotional expressions, extracted from the  
221 NimStim dataset (Tottenham et al., 2009). E-Prime 2.0 software (Schneider, Eschman, &  
222 Zuccolotto, 2002) was used to control and present the stimuli on a screen reflected on a  
223 coil-mounted mirror inside the scanner.

224

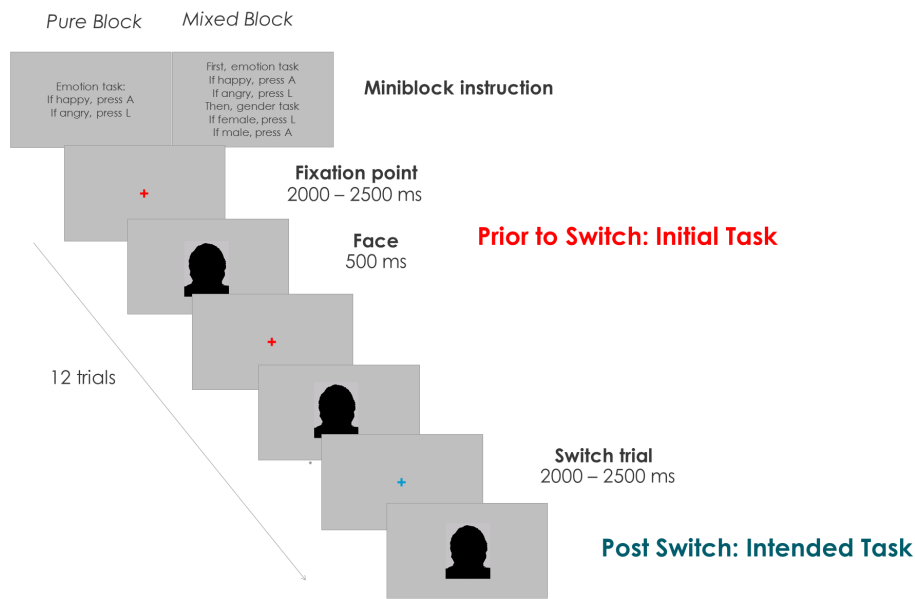
### 225 **2.3. Design and procedure**

226 Participants had to perform a series of categorization tasks where they judged either the  
227 emotion (happy vs. angry), the gender (female vs. male) or the race (black vs. white) of  
228 series of facial displays. These tasks were arranged in miniblocks, which could each  
229 contain one (Pure Miniblock; PM) or two sequential categorization tasks (Mixed  
230 Miniblock; MM). At the beginning of each miniblock, participants received instructions  
231 indicating the number of tasks to perform (1 vs. 2) and their order and nature (Emotion,

232 Gender and/or Race), as well as the key-response mappings. Thus, for PMs, the initial  
233 instruction indicated the one task that had to be performed during the whole miniblock.  
234 Conversely, for MMs, the instruction indicated two tasks, where the participant had to  
235 change from the first to the second task at a certain point of the miniblock. After the  
236 instruction, a coloured (blue or red) fixation point appeared on the screen, followed by a  
237 facial display (see Figure 1). Participants were told that, during MMs, they had to switch  
238 tasks when the fixation changed its colour (from blue to red or vice versa). Once it  
239 switched, they had to continue doing the second task until the end of the miniblock. To  
240 equate the perceptual conditions across blocks, the fixation colour also changed during  
241 PMs, although participants were told to ignore this change.

242

243 Hence, in each MM there was an initial task (first task to perform), an intended task  
244 (second task to perform) and an ignored task (non-relevant for that miniblock).  
245 Importantly, our main fMRI analyses focused on the period before the switch, while  
246 participants needed to represent both the initial task and the intended one. Task switches  
247 were evenly spaced across the miniblock, from trial 1 to 12. This allowed us to decorrelate  
248 brain activity associated with the pre-switch period, post-switch period, and the switch  
249 itself. In total, there were 9 different types of miniblocks: 3 pure (emotion[EE],  
250 gender[GG], race[RR]) and 6 mixed (emotion-gender[EG], emotion-race[ER], gender-  
251 emotion[GE], gender-race[GR], race-emotion[RE], race-gender[RG], see Figure 2).  
252 Across the experiment, pure miniblocks appeared 8 times each, while every type of mixed  
253 miniblock was repeated 12 times. The presentation order of the miniblocks and the  
254 assignment of response options (left or right index) were counterbalanced within each  
255 run. Additionally, to avoid response confounds in the analyses, response mappings  
256 changed between runs. Thus, for each participant odd and even runs had the opposite  
257 response mappings.

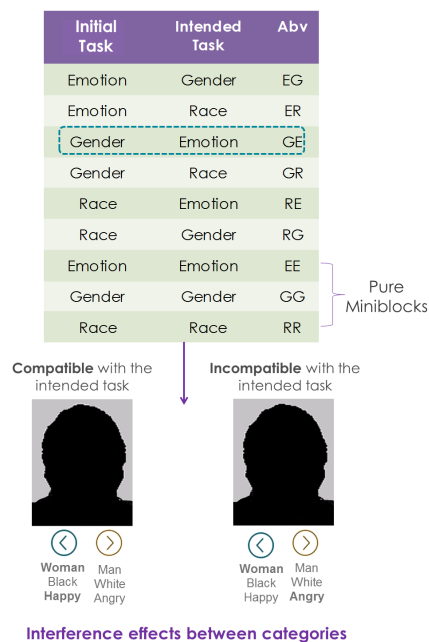


258

259 **Figure 1.** Display of the paradigm (face stimuli are obscured in the preprint version).

260 Example of a miniblock and sequence of trials. Inter-trial-interval (ITI) duration = 2-2.5 s.

261



262

263 **Figure 2.** Top: All possible combinations of miniblocks, depending on the initial and

264 intended tasks, and their abbreviation (Abv). Bottom: Example of interference between

265 initial and intended categories in a Gender-Emotion (GE) miniblock.

266

267 Participants performed a practice block to learn the different tasks and the response  
268 mappings. They were required to obtain a minimum of 80% accuracy at this practice  
269 block prior to entering the scanner. The sequence of each miniblock was as follows: First,  
270 the instruction slide presented the task/s to perform (Pure: 1, Mixed: 2), and the response  
271 mappings (right/left index), during 5 s. Then, a sequence of 12 trials appeared. In each of  
272 them, a fixation point (blue or red, counterbalanced) lasting 2-2.5 s (inter-trial-interval;  
273 ITI; in units of 0.25 s, randomly assigned to each fixation) was followed by a facial  
274 display of 0.5 s. The fixation for the switch trial lasted on average 2.24 s (SD = 0.022; all  
275 participants within a range of  $\pm 2.5$  standard deviations). The experiment consisted of  
276 1152 trials, arranged in 96 miniblocks (72 mixed and 24 pure), distributed in 12 scanning  
277 runs. Hence, each run consisted of 8 miniblocks (6 mixed and 2 pure). Each type of  
278 miniblock was repeated 12 times, once per run, and each time the switch occurred on a  
279 different trial. Presentation order and switch point were counterbalanced through the  
280 experiment, to ensure that each switch occurred on every possible trial for each type of  
281 miniblock and that each identity was associated the same number of times with the switch.  
282 In total, the fMRI task lasted for 60.8 min.

283

284 In addition, we also studied the interference between tasks. Since in MMs the participant  
285 had to perform two tasks sequentially, the established stimulus-response association  
286 could be compatible or incompatible between the current and intended task, depending  
287 on the specific target face. For instance, the gender task could have a stimulus-response  
288 (S-R) association of female-left/male-right and the S-R in the emotion task might be  
289 happy-left/angry-right. Therefore, in a GE miniblock, during the gender task, participants  
290 could encounter happy female faces (both the initial gender and intended emotion tasks  
291 would require the same response: left) or angry female faces (the initial gender task would

292 lead to response with the left index and the emotion with the right one). Thus, the former  
293 would be an example of compatibility between initial and intended tasks, whereas the  
294 latter would entail incompatibility (see Figure 2).

295

## 296 **2.4. Image acquisition and preprocessing**

297 Volunteers were scanned with a 3T Siemens Magnetom Trio, located at the Mind, Brain  
298 and Behavior Research Center (CIMCYC) in Granada, Spain. Functional images were  
299 obtained with a T2\*-weighted echo planar imaging (EPI) sequence, with a TR of 2.210 s.  
300 Forty descending slices with a thickness of 2.3 mm (20% gap) were extracted (TE = 23  
301 ms, flip angle = 70 °, voxel size of 3x3x2.3 mm). The sequence was divided into 12 runs,  
302 consisting of 152 volumes each. Afterwards, an anatomical image for each participant  
303 was acquired using a T1-weighted sequence (TR = 2500 ms; TE = 3.69 ms; flip angle =  
304 7°, voxel size of 1 mm<sup>3</sup>). MRI images were preprocessed and analysed with SPM12  
305 software (<http://www.fil.ion.ucl.ac.uk/spm/software/spm12>). The first 3 images of each  
306 run were discarded to allow the stabilization of the signal. The volumes were realigned  
307 and unwarped and slice-time corrected. Then, the realigned functional images were  
308 coregistered with the anatomical image and were normalized to 3 mm<sup>3</sup> voxels using the  
309 parameters from the segmentation of the anatomical image. Last, images were smoothed  
310 using an 8 mm Gaussian kernel, and a 128 high-pass filter was employed to remove low-  
311 frequency artefacts. Multivariate analyses used non-normalized and non-smoothed data  
312 (Bode & Haynes, 2009; Gilbert & Fung, 2018; Woolgar et al., 2011a, 2011b).

313

## 314 **2.5. fMRI analyses**

### 315 **2.5.1. Univariate**

316 First, we employed a univariate approach to examine the effect of context demands (one  
317 vs. two sequential tasks) and task switching. Our model contained, for each run, one

318 regressor for the instruction of each miniblock, four regressors corresponding to the two  
319 types of miniblock (pure/mixed) with separate regressors for the pre-switch and post-  
320 switch periods, one for the change in fixation colour during mixed miniblocks (indicating  
321 a switch event), one for the change in fixation colour during pure miniblocks (serving as  
322 a baseline for the switch events), and another one for the errors. Both instruction and  
323 miniblock regressors were modelled as a boxcar function with the duration of the entire  
324 pre/post switch period or instruction duration (5 s). Errors were modelled including the  
325 duration of the face of that trial and the following fixation (2.5-3 s). Switch trials were  
326 modelled as events, with stick functions with zero duration locked at the switch in colour  
327 of the fixation point. This provided a model with a total of 8 regressors per run. At the  
328 group level, t-tests were carried out for comparisons related to the effect of task demands  
329 (one vs. two tasks) at the period prior to the switch, and also to compare switching cost  
330 effects (switch trial in the mixed block > switch trial in pure blocks). We report clusters  
331 surviving a family-wise error (FWE) cluster-level correction at  $p < .05$  (from an initial  
332 uncorrected threshold  $p < .001$ ). Additionally, we also performed nonparametric  
333 inference (see Supplementary Materials).

334

### 335 2.5.2. Multivariate analysis

336 We performed multivoxel pattern analyses (MVPA) to examine the brain areas  
337 maintaining the representation of A) current-active initial tasks, and B) intended tasks.  
338 These analyses examined brain activity during the pre-switch period only (although  
339 additional, exploratory analyses were also performed on the post-switch period, see the  
340 Supplementary Materials). Following a Least-Squares Separate Model approach (LSS;  
341 Turner, 2010) we modelled each miniblock (EG, ER, GE, GR, RE, RG) during the period  
342 prior to the switch separately. This method helps to reduce collinearity between regressors  
343 (Abdulrahman & Henson, 2016), by fitting the standard hemodynamic response to two

344 regressors: one for the current event (a type of miniblock prior to the switch) and the  
345 second one for all the remaining events. As in the univariate approach, each miniblock  
346 regressor was modelled as a boxcar function with the duration of the entire pre-switch  
347 period duration.

348

349 The binary classification analyses were performed as follows. First, we classified a)  
350 between any two initial tasks while holding the intended task constant, then b) between  
351 any two intended tasks while holding the initial task constant. For instance, in case a) we  
352 contrasted initial gender task vs. initial race task when the intended task was emotion (GE  
353 vs. RE), and also intended gender vs. intended emotion task when the intended task was  
354 race (ER vs. GR), and intended emotion task vs. intended race task when the intended  
355 task was gender (EG vs. RG). We then averaged decoding accuracies across these  
356 analyses, which indicate whether a particular brain region shows different patterns of  
357 activity depending on what the initial, currently-active task set is, holding the intended  
358 task constant. Conversely, in case b), we compared intended gender vs. intended race  
359 when the initial, currently-active task was emotion (EG vs. ER), intended gender vs.  
360 intended emotion when the initial, currently-active task was race categorization (RE vs.  
361 RG) and intended emotion vs. intended race when the initial, currently-active task was  
362 gender (GE vs. GR). As above, we averaged across these analyses, which indicate  
363 whether a particular brain region shows different patterns of activity depending on what  
364 the intended task set is, holding the currently-performed task constant.

365

366 To carry out these analyses, we performed a whole brain searchlight (Kriegeskorte,  
367 Goebel, & Bandettini, 2006) on the realigned images employing the Decoding Toolbox  
368 (TDT; Hebart, Gorgen, & Haynes, 2015) and custom-written MATLAB code. We created  
369 4-voxel radius spheres and for each sphere, a linear support vector machine classifier (C

370 =1; Pereira, Mitchell, & Botvinick, 2009) was trained and tested using a leave-one-out  
371 cross-validation. Due to the nature of the paradigm and the counterbalancing, once in  
372 each block the switch took place at the first trial (here participants only performed the  
373 intended task). Thus, there was an example of each type of miniblock before the switch  
374 in only 11 runs, differently for each participant and miniblock (i.e. a participant could  
375 lack miniblock EG in run 4 and miniblock RG in run 11). To avoid potential biases in the  
376 classifier for having only one of the classes in a run, for each participant and comparison,  
377 we performed the classification only in the 10 runs where there was an example of both  
378 miniblocks. Resulting from this procedure, we employed the data from 10 scanning runs  
379 (training was performed with data from 9 runs and tested on the remaining run, in an  
380 iterative fashion). In the exceptional case (twice for each contrast in the total sample)  
381 where the two miniblocks in the classification were absent in the same run, classification  
382 was performed on the remaining 11 runs (training with data from 10 runs and testing on  
383 the remaining run). In addition, we observed biases in the decoding estimates when the  
384 switch trial from one of the conditions in the test set matched the opposite class in the  
385 training set, which happened for every comparison in approximately half of the cross-  
386 validation steps. To avoid the biases resulting from this, we additionally removed those  
387 runs where the switch position matched the test from the training set for that specific  
388 cross-validation step.

389

390 Next, we averaged the accuracy maps for a) and b) to obtain a mean classification map  
391 collapsing across initial and intended tasks. This allowed us to detect regions that  
392 contained information about either initial or intended tasks (or both). It also allowed us to  
393 define ROIs that could be used to compare decoding accuracies for initial versus intended  
394 task-sets, in a manner that was unbiased between the two types of information. We

395 additionally conducted whole-brain analyses investigating decoding of the initial task  
396 only, decoding of the intended task only, and the comparisons between the two.

397

398 Afterwards, group analyses were performed by doing one-sample t-tests after normalising  
399 (same as for the univariate analyses) and smoothing the individual accuracy maps (4 mm  
400 Gaussian kernel, consistent with earlier MVPA studies such as Gilbert, 2011; Gilbert &  
401 Fung, 2018). Results were considered significant if they passed an FWE cluster-level  
402 correction at  $p < .05$  (based on an uncorrected forming threshold of  $p < .001$ ). This  
403 statistical approach is consistent with recent MVPA studies (Gilbert & Fung, 2018;  
404 Loose, Wisniewski, Rusconi, Goschke, & Haynes, 2017). We additionally carried out  
405 nonparametric inference (see Supplementary Materials).

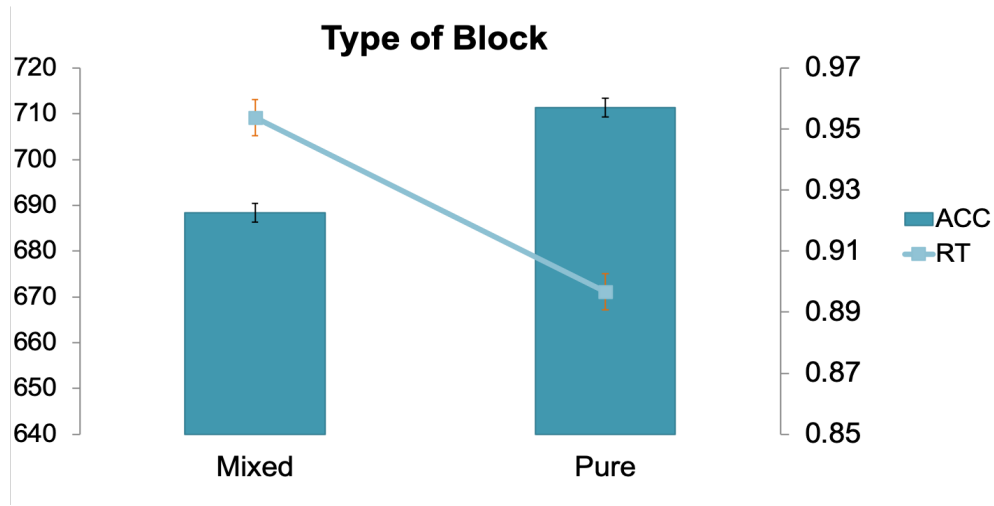
406

### 407 **3. Results**

#### 408 **3.1. Behaviour**

409 First, to study how the number of tasks influenced performance, we performed a paired  
410 t-test on both accuracy and reaction times (RTs), between the two types of Miniblock  
411 (Mixed/Pure), collapsing over pre- and post-switch periods (see Figure 3). Here,  
412 responses were more accurate for pure ( $M = 95.7\%$ ,  $SD = 4.3$ ), than for mixed miniblocks  
413 ( $M = 92.3\%$ ,  $SD = 3.6$ ),  $t_{31} = 5.39$ ,  $p < .001$ , whereas they were faster for pure ( $M = 671.12$   
414 ms,  $SD = 126.3$ ) than for mixed ( $M = 709.18$  ms,  $SD = 142.39$ ) miniblocks,  $t_{31} = 4.83$ ,  
415  $p < .001$ .

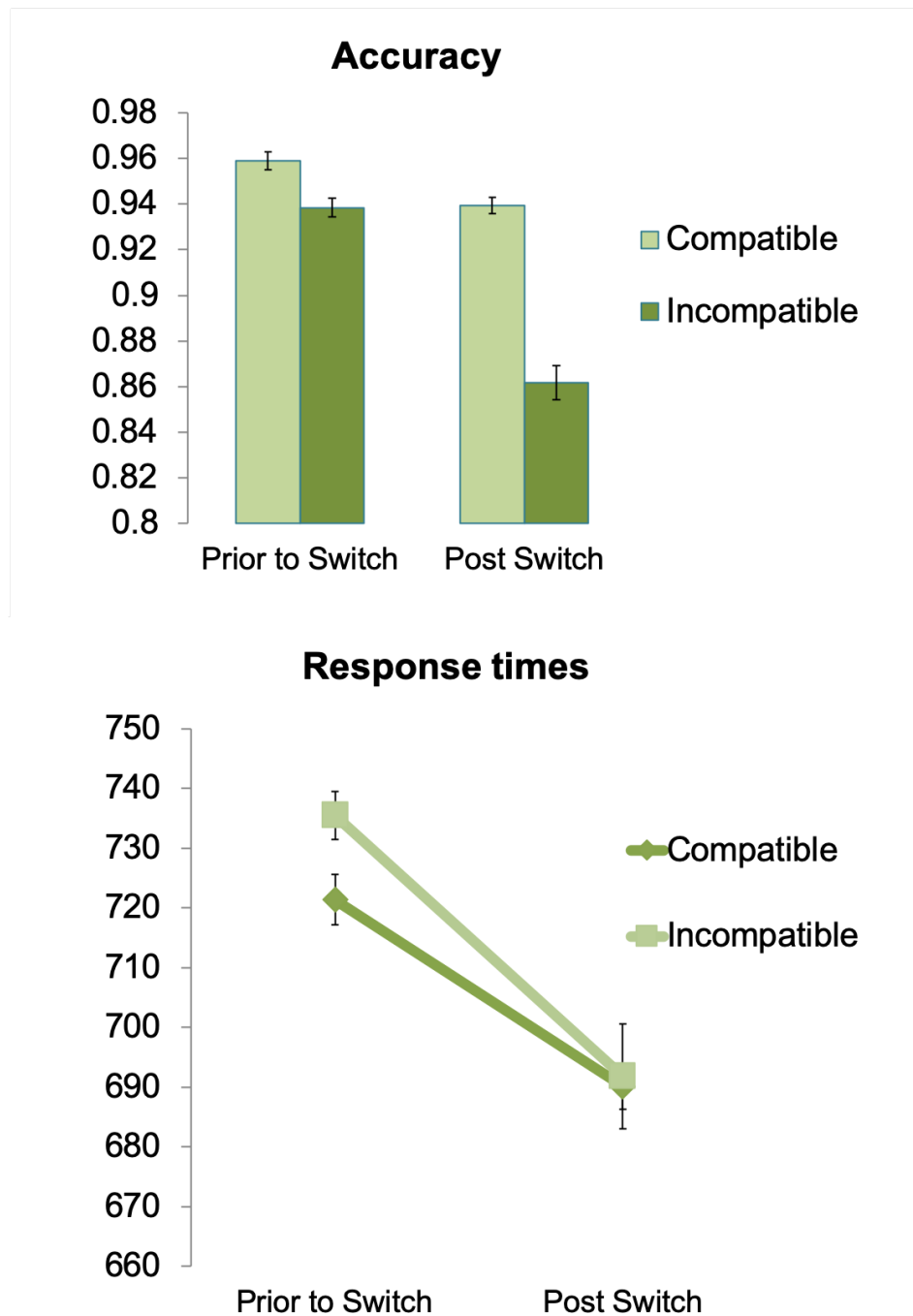
416



417

418 **Figure 3.** Influence of the type of block on performance. Error bars represent within-  
419 subjects 95% confidence intervals (Cousineau, 2005).

420



421

422 **Figure 4.** Interference effects between initial and intended tasks before and after the  
423 switch (MMs). Top: Accuracy rates. Bottom: Reaction times (ms). Error bars represent  
424 within-subjects 95% confidence intervals (Cousineau, 2005).

425

426 In addition, we examined if the intended task influenced initial task performance, and  
427 vice versa. For this, we selected only the mixed miniblocks and entered them into a  
428 repeated measures (rm) ANOVA, with Task (Emotion/Gender/Race), Period of the

429 miniblock (Prior to/Post Switch), and Interference (Compatible/Incompatible) between  
430 initial and intended tasks. Note here that even if we did not have any specific hypothesis  
431 about the influence of the variable Task on performance, we included it as a factor in this  
432 second ANOVA to examine whether the Task modulated the effect of the other two  
433 variables of interest: Period of the block and Interference. Moreover, we refer to initial  
434 and intended as the tasks performed before and after the switch, respectively, to preserve  
435 consistency in the terminology throughout the entire manuscript. In addition, we refer as  
436 compatible trials when the correct response for the initial task-relevant dimension was  
437 associated with the same response for the intended dimension (see an example in Figure  
438 1, right), and incompatible trials when the response associated with the initial task-  
439 relevant dimension interfered with the responses associated with the intended one.  
440 Similarly, after the switch, when the intended task was being performed, compatible trials  
441 referred to those where the correct responses for this task were associated with the same  
442 response for the previous initial task, and incompatible trials when the response associated  
443 with both dimensions differed. This way we could use interference effects as an indicator  
444 of the maintenance of the intended response dimensions during performance.  
445  
446 Accuracy did not show any main effect of Task ( $F < 1$ , see Figure 4). However, we  
447 observed a main effect of Period of the miniblock,  $F_{1,31} = 58.215$ ,  $p < .001$ ,  $\eta_p^2 = .653$ ,  
448 where participants responded more accurately before ( $M = 94.86\%$ ,  $SD = 3.6$ ) than after  
449 the task switch ( $M = 90.05\%$ ,  $SD = 5.4$ ). There was also a main effect of Interference,  
450  $F_{1,31} = 101.83$ ,  $p < .001$ ,  $\eta_p^2 = .767$ , where accuracy was higher for compatible ( $M =$   
451  $94.91\%$ ,  $SD = 4.76$ ) than for incompatible trials ( $M = 90\%$ ,  $SD = 6.79$ ). The interaction  
452 Task x Period was significant,  $F_{2,62} = 3.831$ ,  $p = .029$ ,  $\eta_p^2 = .110$ , showing that  
453 performance was better before than after the switch for all three tasks (all  $F_s > 15$ ,  $p_s <$   
454  $.001$ ), but this difference was larger for the gender task ( $\eta_p^2 = .679$ ). Similarly, the

455 interaction of Period x Interference was significant,  $F_{1,31} = 52.244$ ,  $p < .001$ ,  $\eta_p^2 = .106$ ,  
456 where accuracy was worse for incompatible compared to compatible trials (both  $F_s > 19$ ,  
457  $p_s < .001$ ), but this pattern was more pronounced after ( $F_{1,31} = 107.08$ ,  $p < .001$ ) than before  
458 the switch ( $F_{1,31} = 19.21$ ,  $p < .001$ ). No other interactions reached significance ( $p > .061$ ).  
459  
460 RTs showed (see Figure 4) a main effect for Task ( $F_{2,62} = 24.08$ ,  $p < .001$ ,  $\eta_p^2 = .437$ ),  
461 where race was performed faster ( $M = 691.16$ ,  $SD = 150.07$ ), followed by gender ( $M =$   
462  $709.29$ ,  $SD = 147.11$ ), and emotion ( $M = 728.59$ ,  $SD = 144.14$ ). In addition, we also  
463 observed a main effect of Period ( $F_{1,31} = 32.83$ ,  $p < .001$ ,  $\eta_p^2 = .514$ ), as participants were  
464 faster after ( $M = 690.94$ ,  $SD = 143.38$ ) than prior to the switch ( $M = 728.42$ ,  $SD = 155.72$ ).  
465 Further, we found a main effect of Interference,  $F_{1,31} = 4.829$ ,  $p = .036$ ), where participants  
466 were faster for compatible ( $M = 705.51$ ,  $SD = 147.79$ ) than incompatible trials ( $M =$   
467  $713.65$ ,  $SD = 146.42$ ). An interaction Period x Interference ( $F_{1,32} = 24.08$ ,  $p = .033$ ,  $\eta_p^2 =$   
468  $.437$ ) showed that this interference effect was significant before the switch ( $F_{1,31} = 8.15$ ,  
469  $p = .008$ ), but not after ( $F_{1,31} = .178$ ,  $p > .67$ ). None of the other interactions were significant  
470 ( $p > .2$ ).

471

472 During mixed blocks we observed higher accuracies and reaction times during the period  
473 before the switch and the opposite pattern (low accuracies and faster responses) after it,  
474 which could indicate a trade-off in the data. To address this possibility, we additionally  
475 performed Pearson correlations between mean accuracy and reaction times during both  
476 periods of the miniblock. Results show no association between the two measures, neither  
477 before ( $r = .07$ ;  $p > .35$ ) or after ( $r = .17$ ,  $p > .17$ ) the switch.

478

## 479 **3.2. fMRI**

### 480 3.2.1. Univariate

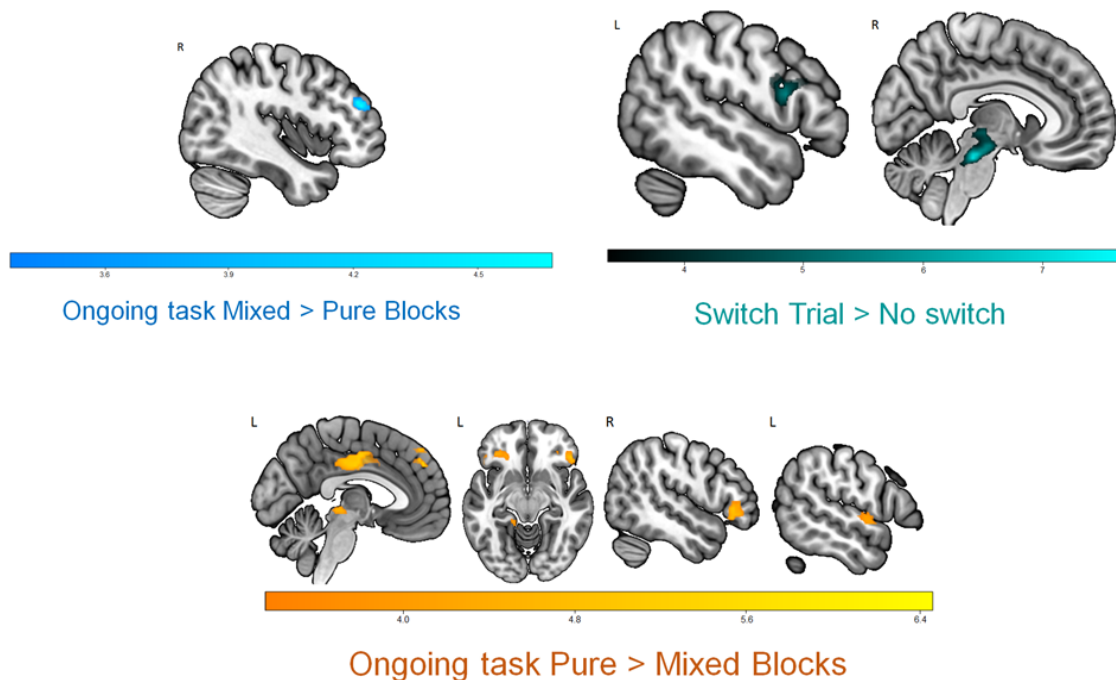
481 3.2.1.1. *Pure vs. Mixed blocks*

482 Before the switch, the right middle frontal gyrus ( $k = 56$ ; MNI coordinates of peak voxel:  
483 42, 44, 23) showed higher activation when participants had to maintain two tasks vs. one  
484 (Mixed > Pure blocks). Conversely, in this scenario, we observed decreased activation  
485 (Pure > Mixed blocks) in a set of regions. These included the bilateral middle cingulate  
486 cortex ( $k = 251$ ; -3, -10, 33), bilateral medial prefrontal cortex (mPFC;  $k = 80$ ; -6, 44, 41),  
487 left orbitofrontal cortex (OFC;  $k = 117$ ; -33, 32, -16), right inferior frontal gyrus  
488 (IFG)/OFC ( $k = 168$ ; 54, 32, -1), left lingual and parahippocampal gyri ( $k = 148$ ; -9, 52,  
489 5) and left superior temporal gyrus ( $k = 62$ ; -57, -1, -4).

490

491 3.2.1.2. *Switch vs. non-switch trials*

492 Transient activity during task switching was observed in the bilateral brainstem and  
493 thalamus ( $k = 291$ ; -3, -28, -22) as well as in a cluster including the left inferior/middle  
494 frontal gyrus (IFG/MFG) and precentral gyrus ( $k = 160$ ; -51, 11, 17).



495

496 **Figure 5.** Univariate results. Effect of task demands (one vs. two) and task switching.  
497 Scales reflect peaks of significant t-values ( $p < .05$ , FWE-corrected for multiple  
498 comparisons).

499

### 500 3.2.1.3. *Interference effects*

501 We assessed whether the interference effects observed on behaviour were matched at a  
502 neural level, by comparing incompatible vs. compatible trials before and after the switch.

503 For this model, we included in each run one regressor for the instruction of each  
504 miniblock, one regressor corresponding to all Pure Miniblocks, four regressors  
505 corresponding to Compatible/Incompatible trials in Mixed Miniblocks, with separate  
506 regressors for the pre-switch and post-switch periods (onset at face presentation) and a

507 last regressor for errors. Instructions and errors were modelled as described in section  
508 2.5.1 Univariate analysis. Pure Miniblocks were modelled as a boxcar function with the  
509 duration of the entire pre/post switch period, while the four remaining regressors  
510 (Compatible Pre, Compatible Post, Incompatible Pre, Incompatible Post) were modelled  
511 as events with zero duration. This provided a model with a total of 7 regressors per run.

512 At the group level, t-tests were carried out for comparisons related to the effect of  
513 Interference before and after the switch. No effect survived multiple comparisons.  
514 However, at a more lenient threshold ( $p < .001$ , uncorrected), data showed higher  
515 activation in the left IFG ( $k = 22$ ;  $-48, 35, 20$ ) for incompatible  $>$  compatible trials. The  
516 opposite comparison (compatible  $>$  incompatible before the switch) or incompatible vs.  
517 compatible contrasts after the switch did not yield any significant results.

518

### 519 3.2.2. Decoding results

520 First, we averaged all individual classification maps to examine the regions sensitive to  
521 any kind of task (initial or intended) during the period prior to the switch. We found that

522 the rostromedial PFC/orbitofrontal cortex (OFC) presented significant accuracies above  
523 chance ( $k = 68; 15, 56, -10$ ). To further examine whether one of the tasks dominated the  
524 classification, we extracted the decoding values from the initial and intended  
525 classification from the general decoding ROI above. A paired t-test between the initial  
526 and intended task decoding values showed no differences between decoding accuracy for  
527 the two types of information,  $t_{31} = .846, p = .404$ . To further test this idea, we ran an ROI  
528 analysis in this region to see whether decoding accuracy was significant for both the initial  
529 and intended task. To avoid non-independency, we employed a Leave-One-Subject-Out  
530 (LOSO) cross-validation approach (Esterman & Yantis, 2010) to select the ROI per  
531 participant. That is, data from each participant was extracted from an ROI that was  
532 defined based on the data from all the other participants, to avoid ‘double dipping’  
533 (Kriegeskorte, Simmons, Bellgowan, & Baker, 2009). After this, both the initial and  
534 intended decoding values showed significant accuracy above chance (1-tailed,  $t_{31} = 3.018,$   
535  $p=.0025$  and  $t_{31} = 2.299, p = .0145$ , respectively). This suggests that the mPFC/OFC  
536 region, prior to the switch, carries information about the relevant tasks to perform,  
537 regardless of whether they are initial or intended.

538

539 To further characterise the information represented in the mPFC/OFC region, we  
540 additionally examined whether we could cross-classify between the initial and intended  
541 tasks, which speaks to the potential overlap between these representations. Therefore, we  
542 performed ROI cross-classification analysis (Kaplan, Man, & Greening, 2015) in the  
543 mPFC/OFC region from the general decoding. We followed the same classification  
544 procedure as described in the methods section, but training the classifier on the initial task  
545 and testing on the intended task, and vice versa. Note that in this scenario the cross-  
546 classification was carried out in a totally independent and orthogonal analysis to that  
547 employed to define the OFC region. However, results showed no significant cross-

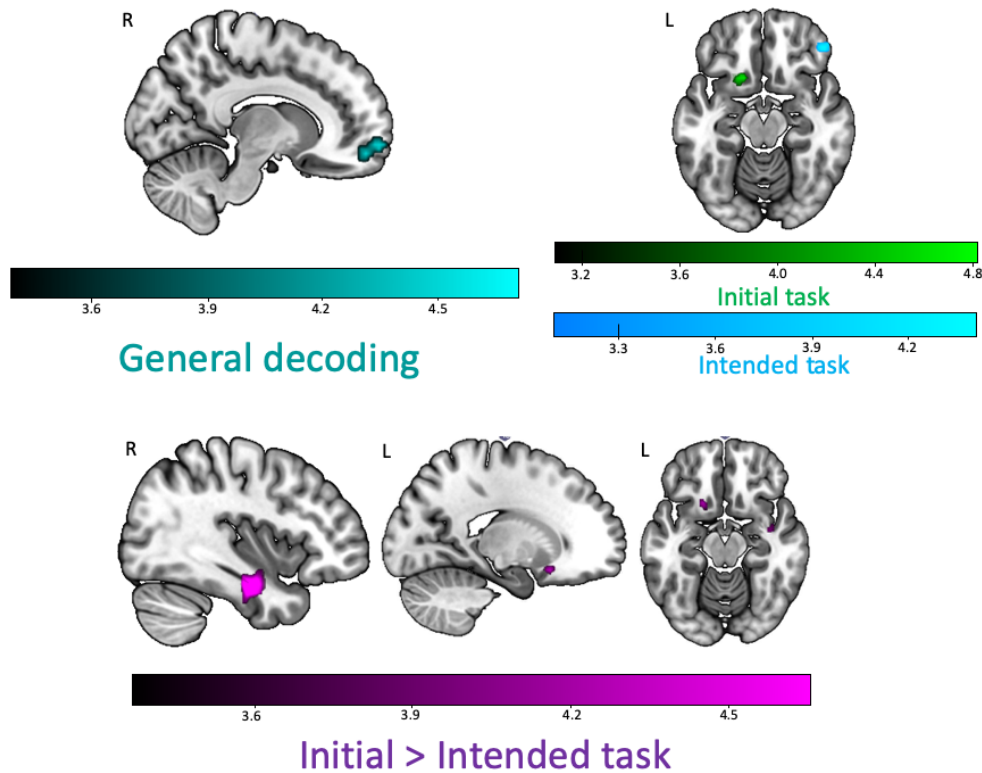
548 classification in this region,  $t_{31} = 1$ ,  $p > .3$ , which suggests that the initial vs. intended  
549 nature of the tasks may change their representational format.

550

551 Moreover, we examined the initial and intended individual classification maps separately  
552 to examine the regions sensitive to each type of task (initial or intended). With this, the  
553 classification of the initial task alone showed a different cluster in the left OFC ( $k = 52$ , -  
554 15, 17, -13). Conversely, we observed the right IFG ( $k = 53$ , 45, 41, -16) for the  
555 classification of the intended task alone. Last, when comparing decoding accuracies  
556 between the initial and intended tasks (subtracting initial – intended accuracy maps), we  
557 observed significantly higher accuracies for the representation of the initial (vs. intended)  
558 in the right FG and the hippocampus ( $k = 148$ ; 39, -13, -25) and also in left OFC ( $k = 44$ ;  
559 -18, 17, -16). However, the opposite contrast (intended vs. initial) did not show any cluster  
560 with significant differences.

561

562 Importantly, these MVPA results were unlikely to be due to differences in response times  
563 (see Supplementary Materials “*RT analyses between miniblock pairs and correlation*  
564 *with decoding accuracies*”).



565

566 **Figure 6.** Multivariate results during the period prior to the switch. Top left: General  
567 decoding (cyan) of the region sensitive to any kind of task (initial or intended). Top right:  
568 Decoding of the initial (green) and intended (blue) task separately. Bottom: Decoding of  
569 initial > intended task (violet). Scales reflect peaks of significant t-values ( $p < .05$ , FWE-  
570 corrected for multiple comparisons).

571

572 Last, although the main focus of this work is the period before the switch, we performed  
573 exploratory classification analysis in the period after the switch to obtain further  
574 understanding about how information is represented once the initial task is no longer  
575 active. Following the same procedure as in section 2.5.2 *Multivariate analysis*, we carried  
576 out the decoding analysis with regressors of interest corresponding to the period after the  
577 switch. As in the previous analyses, we first averaged all individual classification maps  
578 to examine the regions sensitive to any kind of task during the period after the switch.  
579 Here, we observed a cluster in left middle frontal/precentral gyrus ( $k = 61$ ; -36, 11, 35)

580 with significant accuracies above chance. Next, we averaged the classification maps  
581 separately for the currently-active post-switch task and the previously-performed initial  
582 task, to examine the regions sensitive to each type of task. The initial task could be  
583 decoded from bilateral IFG (left;  $k = 48$ ; -54, 29, 26/right;  $k = 45$ ; 54, 32, 5). Conversely,  
584 decoding of the currently-active post-switch task could only be observed at a more liberal  
585 threshold ( $p < .01$ ,  $k = 100$ ) in a cluster including the FG/cerebellum ( $k = 109$ ; 15, -52, -  
586 19) and in left middle/inferior frontal gyrus ( $k = 122$ ; -45, 8, 35).

587

#### 588 **4. Discussion**

589 The present work aimed to examine the representation of A) currently-active, initial task  
590 sets, and B) intended task sets applied to social stimuli during a dual-sequential social  
591 categorization of faces. We found some regions from which we could decode only the  
592 currently-active or the intended task set, along with a region of vmPFC/OFC containing  
593 both types of information although cross-classification between the two was not possible.

594

595 The paradigm employed revealed behavioural costs due to the maintenance of intended  
596 task sets. Here, mixed blocks presented slower responses and lower accuracies, compared  
597 to pure ones, in line with previous studies (Los, 1996; Mari-Beffa et al., 2012). Response  
598 times were slower before than after the switch, when the intended task needed to be held  
599 while performing the initial one, in line with Smith (2003). These results reflect the higher  
600 demands associated with the maintenance of two relevant task sets. In addition, people  
601 need more time to respond when they hold the intention while performing the initial task,  
602 but not after, when they only need to focus on a single task. Further, we aimed to examine  
603 the activation of both initial and intended task sets before the switch by looking at possible  
604 interference between them. Behavioural results showed incompatibility effects in  
605 performance when participants needed to hold the intended task set while performing the

606 ongoing task. These results point to the maintenance of intended task settings, showing  
607 that information about the pending set is maintained online during performance of the  
608 ongoing task.

609

610 Turning to brain activation data, the behavioural costs we observed during the  
611 maintenance of two task sets during mixed blocks were accompanied by increased  
612 activation in the right MFG, while regions such as the left IFG and the thalamus increased  
613 their activation during switching trials. Incompatible trials during this period were also  
614 related to activation in left IPFC, but only at an uncorrected statistical threshold. These  
615 results fit with previous work that associated IPFC with sustained control during dual  
616 tasks (Braver et al., 2003; Szameitat et al., 2002) and the maintenance of delayed  
617 intentions (Gilbert, 2011). Lateral PFC has also an important role in rule representation  
618 and the selection of correct rules (Brass & Cramon, 2002; Crone, Wendelken, Donohue,  
619 & Bunge, 2006), while the thalamus has also shown a role in cognitive flexibility during  
620 task switching (Rikhye, Gilra, & Halassa, 2018). Overall, this pattern reflects the  
621 cognitive demands of holding two tasks in mind, extending the results to the maintenance  
622 of social categorization sets.

623

624 In addition, we observed a set of task-negative regions such as mPFC, middle cingulate,  
625 OFC, IFG and temporal cortex which showed reduced signal when participants needed to  
626 hold an intended task set. Similarly, Landsiedel & Gilbert (2015) carried out an intention-  
627 offloading paradigm where participants had to remember a delayed intention, which they  
628 had to fulfil after a brief filled delay. During the maintenance of such intention they found  
629 a set of deactivated regions including mPFC, posterior cingulate cortex, infero-temporal  
630 cortex, and temporo-parietal cortex. Interestingly, these authors showed that when  
631 participants had the opportunity to offload intentions by setting an external reminder, this

632 decrease of activation was ameliorated. This reduction suggests that these task-negative  
633 areas play a role in the representation of the delayed tasks. Pure blocks in our tasks are  
634 similar to the offloading condition in Landsiedel & Gilbert (2015), as participants needed  
635 to sustain only the initial task set to perform the correct social categorization. Therefore,  
636 taking these results into account, it seems unlikely that task-negative regions reflect  
637 simply a “default mode” (Fox et al., 2005), but rather that this deactivation is, to some  
638 extent, playing a functional role during task performance (Spreng, 2012).

639

640 Currently, multivariate pattern analyses are one of the most powerful approaches to study  
641 the information contained in different brain areas. In this work, we employed MVPA to  
642 study the regions representing initial and intended task sets. Importantly, a novelty of our  
643 approach was to do so by employing three different tasks instead of just two, unlike most  
644 previous studies (e.g. Haynes et al., 2007; Momennejad & Haynes, 2013). We were able  
645 to distinguish different regions representing initial and intended task sets. The currently-  
646 active initial task was decoded from left OFC, while information about the intended one  
647 was contained in the right IFG. Also, comparing between these two, a nearby OFC region  
648 together with the FG showed higher fidelity of the representation for the initial vs.  
649 intended task set. The left OFC region found for the initial task decoding has been  
650 previously associated with representations of facial information related to social  
651 categories (Freeman, Rule, Adams, & Ambady, 2010) and it also facilitates object  
652 recognition in lower level areas such as the FG (Bar et al., 2006). In addition, the FG  
653 showed greater fidelity of the representation of initial vs. intended task sets, which could  
654 indicate the allocation of attentional resources to process current relevant information in  
655 earlier perceptual regions. Besides having a prominent role in processing faces (Haxby et  
656 al., 2000), previous studies have been able to decode task-relevant information related to  
657 social categories (e.g. female vs. male, black vs. white) in perceptual regions such as the

658 FG (Gilbert et al., 2012; Kaul et al., 2014, 2011; Stolier & Freeman, 2017). On top of  
659 this, previous work using facial stimuli in the field of social perception and prejudice has  
660 shown how the FG is influenced by stereotypical associations and evaluations of social  
661 categories associated with the OFC (Gilbert et al., 2012; Stolier & Freeman, 2016). Our  
662 data fit and extend this work, suggesting that both OFC and FG contain information about  
663 the appropriate task set to perform the initial classification, pointing out the role of both  
664 high and lower-level perceptual regions in the representation of ongoing task sets  
665 performed on facial stimuli.

666

667 Conversely, decoding of the intended task was possible from the IFG. Previous work has  
668 related IPFC with the representation of intentions (Haynes et al., 2007; Momennejad &  
669 Haynes, 2012; Momennejad & Haynes, 2013; Soon et al., 2008) and it has also been  
670 linked to task-set preparation (e.g. González-García, Arco, Palenciano, Ramírez, & Ruz,  
671 2017; González-García, Mas, de Diego-Balaguer & Ruz, 2016; Sakai & Passingham,  
672 2003). This result, however, contradicts the proposal of Gilbert (2011) in which IPFC  
673 would serve as a general store for delayed intentions without information about their  
674 content. Nonetheless, while Gilbert (2011) decoded simpler stimulus-response mappings,  
675 in our study we classified abstract task-set information, as previous studies that also  
676 decoded intention from IPFC did (e.g. Haynes et al., 2007; Momennejad & Haynes,  
677 2013). Therefore, our work agrees with Momennejad & Haynes (2013), suggesting that  
678 IPFC may represent delayed intentions when their content is abstract enough.

679

680 Interestingly, we found a region in vmPFC/OFC that contained information about both  
681 initial and intended task sets. We examined if this vmPFC/OFC region contained  
682 overlapping representations of both initial and intended task sets by performing a cross-  
683 classification analysis, and observed a lack of generalization from the two sets of

684 representations. Our cluster is close to the mPFC region found by previous intention  
685 studies (e.g. Gilbert, 2011), but located in a more ventral area. Notably, in our paradigm  
686 both the initial and intended tasks that participant performed were equally relevant and  
687 were based on the same set of stimuli. Altogether, this suggests that mPFC may be  
688 recruited when relevant task sets need to be held for a period of time, irrespective if this  
689 information is being using at the moment or later. This result also fits with a recent  
690 proposal (Schuck, Cai, Wilson, & Niv, 2016) characterising this region as a repository  
691 for cognitive maps of task states. Specifically, the vmPFC/OFC would represent task-  
692 relevant states that are hard to discriminate based on sensory information alone (Schuck  
693 et al., 2016; Wilson, Takahashi, Schoenbaum, & Niv, 2014), similar to our study. Overall,  
694 this suggests a role for this region in the maintenance of task-relevant information,  
695 regardless of when it is needed. Given that cross-classification between initial and  
696 intended task sets was not possible in this region, this would be compatible with  
697 multiplexed representations of the two types of information (i.e. representations using  
698 orthogonal representational codes). It could also be compatible with nonoverlapping  
699 populations of cells representing initial and intended tasks within the voxels in this region.  
700 Further, it could be argued that the lack of cross-classification between initial and  
701 intended tasks could be explained by differential processes underlying the representation  
702 of these tasks. That is, the initial one could be represented simply by the activation of the  
703 S-R associations, while the intended one would rely on the maintenance of a general task  
704 set. Nonetheless, an explanation relying solely on this distinction seems unlikely, since  
705 we observed interference effects. Even though the interference effect for accuracy was  
706 smaller before the switch, for reaction times we observed interference only during this  
707 period. This indicates that the S-R association for both tasks is active prior the switch,  
708 although there could be some distinctions in the way these response representations are

709 maintained. However, the lack of significant cross-classification could also reflect simply  
710 a lack of statistical power.

711

712 Despite our decoding results, we did not find the dissociation pattern that we predicted  
713 for initial and intended task sets. Although we could decode intended task sets from  
714 mPFC, consistent with previous studies (Gilbert, 2011; Haynes et al., 2007; Momennejad  
715 & Haynes, 2012; Momennejad & Haynes, 2013), we did not find a frontoparietal  
716 representation of initial task sets as previous studies have (Qiao et al., 2017; Waskom et  
717 al., 2014; Woolgar et al., 2011b). This discrepancy could be explained by differences in  
718 the stimuli and task employed. Previous studies have decoded task information in the  
719 form of classification between different stimulus-responses mappings or different types  
720 of stimuli. In contrast, in our task we employed the same stimuli for all tasks, and the  
721 differences between the information to decode relied in the representation of the social  
722 category needed for the specific part of the miniblock, rather than perceptual features (e.g.  
723 the colour or shape of target stimuli), which may be easier to decode (Bhandari, Gagne,  
724 & Badre, 2018).

725

726 To conclude, in the present work we examined the representation of A) currently-active  
727 initial task sets, and B) intended task sets during a social categorization dual-sequential  
728 task. Crucially, we directly examined the common and differential representation of  
729 initial and delayed task sets, extending previous work studying these mechanisms  
730 separately. Moreover, we employed faces as target stimuli to complement prior research.  
731 Apart from replicating previous findings in dual tasks with social stimuli, we show how  
732 task set information was contained in different regions, depending on when it was needed.  
733 Thus, currently-active initial tasks were represented in specialized regions related to face  
734 processing and social categorization such as the OFC and FG, while intended ones were

735 represented in IPFC. On top of that, we showed a common brain region in vmPFC/OFC  
736 maintaining a general representation of task-relevant information, irrespective of when  
737 the task is performed, albeit it is not clear whether overlapping patterns of activation  
738 represent both types of information. Moreover, the results from the classification after the  
739 switch suggest that the representation of the two relevant tasks varies once the switch  
740 takes place and the initial task is no longer active. Future research should further  
741 characterize the representational format of relevant task information depending on when  
742 it is needed and examine the structure of the task set representation within these regions,  
743 for instance using Representational Similarity Analysis (RSA, Kriegeskorte, Mur, &  
744 Bandettini, 2008). Also, studying the interaction of sustained task sets with specific  
745 conditions of each trial would extend our knowledge of the representational dynamics of  
746 current and intended task-relevant information. Last, due to the social significance of  
747 faces, one step forward would be to examine how their representation may vary in social  
748 scenarios, contexts in which faces and other social stimuli are particularly relevant to  
749 guide behaviour (Díaz-Gutiérrez, Alguacil, & Ruz, 2017).

750

### 751 **Funding**

752 This work was supported by the Spanish Ministry of Science and Innovation (PSI2016-  
753 78236-P to M.R.) and the Spanish Ministry of Education, Culture and Sports  
754 (FPU2014/04272 to P.D.G.).

755

### 756 **Acknowledgments**

757 This research is part of P.D.G.'s activities for the Psychology Graduate Program of the  
758 University of Granada.

759

760

761 **References**

- 762 Abdulrahman, H., & Henson, R. N. (2016). Effect of trial-to-trial variability on optimal  
763 event-related fMRI design: Implications for Beta-series correlation and multi-voxel  
764 pattern analysis. *NeuroImage*, *125*, 756–766.  
765 <https://doi.org/10.1016/j.neuroimage.2015.11.009>
- 766 Bar, A. M., Kassam, K. S., Ghuman, A. S., Boshyan, J., Schmid, A. M., Dale, A. M.,  
767 Hämäläinen, M.S., Marinkovic, K., Schacter, D.L., Rosen, B.R., & Halgren, E.  
768 (2006). Top-down facilitation of visual recognition. *Proceedings of the National*  
769 *Academy of Sciences*, *103*(2), 449–454. <https://doi.org/10.1073/pnas.0507062103>
- 770 Bhandari, A., Gagne, C., & Badre, D. (2018). Just above Chance: Is It Harder to Decode  
771 Information from Prefrontal Cortex Hemodynamic Activity Patterns? *Journal of*  
772 *Cognitive Neuroscience*, *30*(10), 1473–1498. <https://doi.org/10.1162/jocn>
- 773 Bode, S., Haynes, J. D. (2009). Decoding sequential stages of task preparation in the  
774 human brain. *Neuroimage*, *45*(2), 606–613.  
775 <http://dx.doi.org/10.1016/j.neuroimage.2008.11.031>.
- 776 Brass, M., & Cramon, D. Y. Von. (2002). The Role of the Frontal Cortex in Task  
777 Preparation. *Cerebral Cortex*, *12*(9), 908–914.  
778 <https://doi.org/10.1093/cercor/12.9.908>
- 779 Braver, T. S., Reynolds, J. R., & Donaldson, D. I. (2003). Neural Mechanisms of  
780 Transient and Sustained Cognitive Control during Task Switching. *Neuron*, *39*(4),  
781 713–726. [https://doi.org/10.1016/S0896-6273\(03\)00466-5](https://doi.org/10.1016/S0896-6273(03)00466-5)
- 782 Buckner, R. L., Andrews-Hanna, J. R., & Schacter, D. L. (2008). The Brain’s Default  
783 Network. *Annals of the New York Academy of Sciences*, *1124*(1), 1–38.  
784 <https://doi.org/10.1196/annals.1440.011>
- 785 Buckner, R. L., & Carroll, D. C. (2007). Self-projection and the brain. *Trends in*  
786 *Cognitive Sciences*, *11*(2), 49–57. <https://doi.org/10.1016/j.tics.2006.11.004>

- 787 Cousineau, D. (2005). Confidence intervals in within-subject designs: A simpler  
788 solution to Loftus and Masson's method. *Tutorials in Quantitative Methods for*  
789 *Psychology, 1(1)*, 42-45. <https://doi.org/10.20982/tqmp.01.1.p042>
- 790 Crittenden, B. M., Mitchell, D. J., & Duncan, J. (2015). Recruitment of the default  
791 mode network during a demanding act of executive control. *ELife, 4:e06481*.  
792 <https://doi.org/10.7554/eLife.06481>
- 793 Crone, E. A., Wendelken, C., Donohue, S. E., & Bunge, S. A. (2006). Neural evidence  
794 for dissociable components of task-switching. *Cerebral Cortex, 16(4)*, 475–486.  
795 <https://doi.org/10.1093/cercor/bhi127>
- 796 Díaz-Gutiérrez, P., Alguacil, S., & Ruz, M. (2017). Bias and control in social decision-  
797 making. In A. Ibáñez, L. Sedeño, & A. Gacriá (Eds.), *Neuroscience and Social*  
798 *Science: The Missing Link* (pp. 47–68). Cham, Switzerland: Springer.  
799 <https://doi.org/10.1007/978-3-319-68421-5>
- 800 Dumontheil, I., Thompson, R., & Duncan, J. (2011). Assembly and Use of New Task  
801 Rules in Fronto-parietal Cortex. *Journal of Cognitive Neuroscience, 23(1)*, 168–  
802 182. <https://doi.org/10.1162/jocn.2010.21439>
- 803 Duncan, J. (2010). The multiple-demand (MD) system of the primate brain: mental  
804 programs for intelligent behaviour. *Trends in Cognitive Sciences, 14(4)*, 172–179.  
805 <https://doi.org/10.1016/j.tics.2010.01.004>
- 806 Elton, A., & Gao, W. (2015). Task-positive Functional Connectivity of the Default  
807 Mode Network Transcends Task Domain. *Journal of Cognitive Neuroscience,*  
808 *27(12)*, 2369–2381. <https://doi.org/10.1162/jocn>
- 809 Esterman, M., & Yantis, S. (2010). Perceptual expectation evokes category-selective  
810 cortical activity. *Cerebral Cortex, 20(5)*, 1245–1253.  
811 <https://doi.org/10.1093/cercor/bhp188>
- 812 Fox, M. D., Snyder, A. Z., Vincent, J. L., Corbetta, M., Essen, D. C. Van, & Raichle,

- 813 M. E. (2005). The human brain is intrinsically organized into dynamic,  
814 anticorrelated functional networks. *Proceedings of the National Academy of*  
815 *Sciences*, 102(27), 9673–9678. <https://doi.org/10.1073/pnas.0504136102>
- 816 Freeman, J. B., Ma, Y., Barth, M., Young, S. G., Han, S., & Ambady, N. (2015). The  
817 neural basis of contextual influences on face categorization. *Cerebral Cortex*,  
818 25(2), 415–422. <https://doi.org/10.1093/cercor/bht238>
- 819 Freeman, J. B., Rule, N. O., Adams, R. B., & Ambady, N. (2010). The neural basis of  
820 categorical face perception: Graded representations of face gender in fusiform and  
821 orbitofrontal cortices. *Cerebral Cortex*, 20(6), 1314–1322.  
822 <https://doi.org/10.1093/cercor/bhp195>
- 823 Gilbert, S. J. (2011). Decoding the Content of Delayed Intentions. *Journal of*  
824 *Neuroscience*, 31(8), 2888–2894. [https://doi.org/10.1523/JNEUROSCI.5336-](https://doi.org/10.1523/JNEUROSCI.5336-10.2011)  
825 10.2011
- 826 Gilbert, S. J., & Fung, H. (2018). Decoding intentions of self and others from fMRI  
827 activity patterns. *NeuroImage*, 172, 278–290.  
828 <https://doi.org/10.1016/j.neuroimage.2017.12.090>
- 829 Gilbert, S. J., Swencionis, J. K., & Amodio, D. M. (2012). Evaluative vs. trait  
830 representation in intergroup social judgments: Distinct roles of anterior temporal  
831 lobe and prefrontal cortex. *Neuropsychologia*, 50(14), 3600–3611.  
832 <https://doi.org/10.1016/j.neuropsychologia.2012.09.002>
- 833 González-García, C., Arco, J. E., Palenciano, A. F., Ramírez, J., & Ruz, M. (2017).  
834 Encoding, preparation and implementation of novel complex verbal instructions.  
835 *NeuroImage*, 148, 264–273. <https://doi.org/10.1016/j.neuroimage.2017.01.037>
- 836 González-García, C., Mas-Herrero, E., de Diego-Balaguer, R., & Ruz, M. (2016). Task-  
837 specific preparatory neural activations in low-interference contexts. *Brain*  
838 *Structure and Function*, 221(8), 3997–4006. [36](https://doi.org/10.1007/s00429-015-</a></p></div><div data-bbox=)

- 839 1141-5
- 840 Hampson, M., Driesen, N. R., Skudlarski, P., Gore, J. C., & Constable, R. T. (2006).  
841 Brain Connectivity Related to Working Memory Performance. *Journal of*  
842 *Neuroscience*, 26(51), 13338–13343. [https://doi.org/10.1523/JNEUROSCI.3408-](https://doi.org/10.1523/JNEUROSCI.3408-06.2006)  
843 06.2006
- 844 Haxby, J. V., Hoffman, E. A., & Gobbini, M. I. (2000). The Distributed Human Neural  
845 System for Face Perception. *Trends in Cognitive Sciences*, 4(6), 223–233.  
846 [https://doi.org/10.1016/S1364-6613\(00\)01482-0](https://doi.org/10.1016/S1364-6613(00)01482-0)
- 847 Haxby, J. V., Connolly, A.C. & Guntupalli, J.S. (2014). Decoding Neural  
848 Representational Spaces Using Multivariate Pattern Analysis. *Annual Review of*  
849 *Neuroscience*, 35, 435–456. [https://doi.org/10.1146/annurev-neuro-062012-](https://doi.org/10.1146/annurev-neuro-062012-170325)  
850 170325
- 851 Haynes, J. D. (2015). A Primer on Pattern-Based Approaches to fMRI: Principles,  
852 Pitfalls, and Perspectives. *Neuron*, 87, 257-270.  
853 <https://dx.doi.org/10.1016/j.neuron.2015.05.025>.
- 854 Haynes, J. D., Sakai, K., Rees, G., Gilbert, S., Frith, C., & Passingham, R. E. (2007).  
855 Reading Hidden Intentions in the Human Brain. *Current Biology*, 17(4), 323–328.  
856 <https://doi.org/10.1016/j.cub.2006.11.072>
- 857 Hebart, M. N., Görgen, K., & Haynes, J. D. (2015). The Decoding Toolbox (TDT): a  
858 versatile software package for multivariate analyses of functional imaging data.  
859 *Frontiers in Neuroinformatics*, 8, 88. <https://doi.org/10.3389/fninf.2014.00088>
- 860 Kanwisher, N., & Yovel, G. (2006). The fusiform face area: A cortical region  
861 specialized for the perception of faces. *Philosophical Transactions of the Royal*  
862 *Society B: Biological Sciences*, 361(1476), 2109–2128.  
863 <https://doi.org/10.1098/rstb.2006.1934>
- 864 Kaplan, J. T., Man, K., & Greening, S. G. (2015). Multivariate cross-classification:

- 865 applying machine learning techniques to characterize abstraction in neural  
866 representations. *Frontiers in Human Neuroscience*, 9:151.  
867 <https://doi.org/10.3389/fnhum.2015.00151>
- 868 Kaul, C., Ratner, K. G., & Van Bavel, J. J. (2014). Dynamic representations of race:  
869 Processing goals shape race decoding in the Fusiform gyri. *Social Cognitive and*  
870 *Affective Neuroscience*, 9(3), 326–332. <https://doi.org/10.1093/scan/nss138>
- 871 Kaul, C., Rees, G., & Ishai, A. (2011). The Gender of Face Stimuli is Represented in  
872 Multiple Regions in the Human Brain. *Frontiers in Human Neuroscience*, 4:238.  
873 <https://doi.org/10.3389/fnhum.2010.00238>
- 874 Kliegel, M., McDaniel, M., & Einstein, G. (2008). *Prospective memory: cognitive,*  
875 *neuroscience, developmental, and applied perspectives*. Mahwah, NJ: Erlbaum.
- 876 Koski, J. E., Collins, J. A., Olson, I. R., & Hospital, G. (2017). The neural  
877 representation of social status in the extended face- processing network. *European*  
878 *Journal of Neuroscience*, 46(12), 2795–2806.  
879 <https://doi.org/10.1111/ejn.13770>.The
- 880 Kriegeskorte, N., Goebel, R., & Bandettini, P. (2006). Information-based functional  
881 brain mapping. *Proceedings of the National Academy of Sciences*, 103, 3863–3868.  
882 <https://doi.org/10.1073/pnas.0600244103>
- 883 Kriegeskorte, N., Mur, M., & Bandettini, P. (2008). Representational similarity analysis  
884 - connecting the branches of systems neuroscience. *Frontiers in Systems*  
885 *Neuroscience*, 2: 4. <https://doi.org/10.3389/neuro.06.004.2008>
- 886 Kriegeskorte, N., Simmons, W. K., Bellgowan, P. S., & Baker, C. I. (2009). Circular  
887 analysis in systems neuroscience: The dangers of double dipping. *Nature*  
888 *Neuroscience*, 12(5), 535–540. <https://doi.org/10.1038/nn.2303>
- 889 Landsiedel, J., & Gilbert, S. J. (2015). Creating external reminders for delayed  
890 intentions: Dissociable influence on “task-positive” and “task-negative” brain

- 891 networks. *NeuroImage*, *104*, 231–240.  
892 <https://doi.org/10.1016/j.neuroimage.2014.10.021>
- 893 Loose, L. S., Wisniewski, D., Rusconi, M., Goschke, T., & Haynes, J.-D. (2017).  
894 Switch-Independent Task Representations in Frontal and Parietal Cortex. *The*  
895 *Journal of Neuroscience*, *37*(33), 8033–8042.  
896 <https://doi.org/10.1523/jneurosci.3656-16.2017>
- 897 Los, S. A. (1996). On the origin of mixing costs: Exploring information processing in  
898 pure and mixed blocks of trials. *Acta Psychologica*, *94*(2), 145–188.  
899 [https://doi.org/10.1016/0001-6918\(95\)00050-X](https://doi.org/10.1016/0001-6918(95)00050-X)
- 900 Mari-Beffa, P., Cooper, S., & Houghton, G. (2012). Unmixing the mixing cost:  
901 Contributions from dimensional relevance and stimulus-response suppression.  
902 *Journal of Experimental Psychology: Human Perception and Performance*, *38*(2),  
903 478–488. <https://doi.org/10.1037/a0025979>
- 904 Mars, R. B., Neubert, F. X., Noonan, M. P., Sallet, J., Toni, I., & Rushworth, M. F.  
905 (2012). On the relationship between the “default mode network” and the “social  
906 brain.” *Frontiers in Human Neuroscience*, *6*, 1–9.  
907 <https://doi.org/10.3389/fnhum.2012.00189>
- 908 Meyer, M. L., Davachi, L., Ochsner, K. N., & Lieberman, M. D. (2018). Evidence That  
909 Default Network Connectivity During Rest Consolidates Social Information.  
910 *Cerebral Cortex*, *29*(5), 1–11. <https://doi.org/10.1093/cercor/bhy071>
- 911 Mitchell, J. P., Macrae, C. N., & Banaji, M. R. (2006). Dissociable Medial Prefrontal  
912 Contributions to Judgments of Similar and Dissimilar Others. *Neuron*, *50*(4), 655–  
913 663. <https://doi.org/10.1016/j.neuron.2006.03.040>
- 914 Momennejad, I., & Haynes, J. D. (2012). Human anterior prefrontal cortex encodes the  
915 “what” and “when” of future intentions. *NeuroImage*, *61*(1), 139–148.  
916 <https://doi.org/10.1016/j.neuroimage.2012.02.079>

- 917 Momennejad, I., & Haynes, J. D. (2013). Encoding of Prospective Tasks in the Human  
918 Prefrontal Cortex under Varying Task Loads. *Journal of Neuroscience*, 33(44),  
919 17342–17349. <https://doi.org/10.1523/JNEUROSCI.0492-13.2013>
- 920 Monsell, S. (2003). Task Switching. *Trends in Cognitive Sciences*, 7(3), 134–140.  
921 [https://doi.org/doi:10.1016/S1364-6613\(03\)00028-7](https://doi.org/doi:10.1016/S1364-6613(03)00028-7)
- 922 Moyes, J., Sari-Sarraf, N., & Gilbert, S. J. (2019). Characterising monitoring processes  
923 in event-based prospective memory: Evidence from pupillometry. *Cognition*, 184,  
924 83–95. <https://doi.org/10.1016/j.cognition.2018.12.007>
- 925 Palenciano, A. F., González-García, C., Arco, J. E., & Ruz, M. (2019). Transient and  
926 Sustained Control Mechanisms Supporting Novel Instructed Behavior. *Cerebral*  
927 *Cortex*, 29, 3948–3960. <https://doi.org/10.1093/cercor/bhy273>
- 928 Palenciano, A. F., González-García, C., Arco, J. E., Pessoa, L. & Ruz, M. (2019).  
929 Representational organization of novel task sets during proactive encoding.  
930 *Journal of Neuroscience*, 39, 0725-19. [https://doi.org/10.1523/JNEUROSCI.0725-](https://doi.org/10.1523/JNEUROSCI.0725-19.2019)  
931 19.2019
- 932 Pereira, F., Mitchell, T., & Botvinick, M. (2009). Machine learning classifiers and  
933 fMRI: A tutorial overview. *NeuroImage*, 45(1), S199–S209.  
934 <https://doi.org/10.1016/j.neuroimage.2008.11.007>
- 935 Qiao, L., Zhang, L., Chen, A., & Egner, T. (2017). Dynamic Trial-by-Trial Recoding of  
936 Task-Set Representations in the Frontoparietal Cortex Mediates Behavioral  
937 Flexibility. *The Journal of Neuroscience*, 37(45), 11037–11050.  
938 <https://doi.org/10.1523/jneurosci.0935-17.2017>
- 939 Raichle, M. (2015). The Brain’s Default Network. *Annals of the New York Academy of*  
940 *Sciences*, 38, 433–447. <https://doi.org/10.1196/annals.1440.011>
- 941 Rikhye, R. V., Gilra, A., & Halassa, M. M. (2018). Thalamic regulation of switching  
942 between cortical representations enables cognitive flexibility. *Nature*

- 943        *Neuroscience*, 21(12), 1753–1763. <https://doi.org/10.1038/s41593-018-0269-z>
- 944    Rogers, R. D., & Monsell, S. (1995). Costs of a predictable switch between simple  
945        cognitive tasks. *Journal of Experimental Psychology: General*, 124(2), 207–231.  
946        <https://doi.org/http://dx.doi.org/10.1037/0096-3445.124.2.207>
- 947    Sakai, K., & Passingham, R. E. (2003). Prefrontal interactions reflect future task  
948        operations. *Nature Neuroscience*, 6(1), 75–81. <https://doi.org/10.1038/nn987>
- 949    Schneider, W., Eschman, A., & Zuccolotto, A. (2002). E-Prime user’s guide. Pittsburgh:  
950        Psychology Software Tools Inc.
- 951    Schuck, N. W., Cai, M. B., Wilson, R. C., & Niv, Y. (2016). Human Orbitofrontal  
952        Cortex Represents a Cognitive Map of State Space. *Neuron*, 91(6), 1402–1412.  
953        <https://doi.org/10.1016/j.neuron.2016.08.019>
- 954    Singer, T., Kiebel, S. J., Winston, J. S., Dolan, R. J., & Frith, C. D. (2004). Brain  
955        Responses to the Acquired Moral Status of Faces. *Neuron*, 41(4), 653–662.  
956        [https://doi.org/10.1016/S0896-6273\(04\)00014-5](https://doi.org/10.1016/S0896-6273(04)00014-5)
- 957    Smith, R. E. (2003). The Cost of Remembering to Remember in Event-Based  
958        Prospective Memory: Investigating the Capacity Demands of Delayed Intention  
959        Performance. *Journal of Experimental Psychology: Learning Memory and*  
960        *Cognition*, 29(3), 347–361. <https://doi.org/10.1037/0278-7393.29.3.347>
- 961    Smith, V., Mitchell, D. J., & Duncan, J. (2018). Role of the Default Mode Network in  
962        Cognitive Transitions, *Cerebral Cortex*, 28(10), 3685–3696.  
963        <https://doi.org/10.1093/cercor/bhy167>
- 964    Soon, C. S., Brass, M., Heinze, H. J., & Haynes, J. D. (2008). Unconscious  
965        determinants of free decisions in the human brain. *Nature Neuroscience*, 11(5),  
966        543–545. <https://doi.org/10.1038/nn.2112>
- 967    Spreng, N. R. (2012). The fallacy of a “task-negative” network. *Frontiers in*  
968        *Psychology*, 3, 1–5. <https://doi.org/10.3389/fpsyg.2012.00145>

- 969 Spreng, R. N., Mar, R. A., & Kim, A. S. N. (2008). The Common Neural Basis of  
970 Autobiographical Memory, Prospection, Navigation, Theory of Mind, and the  
971 Default Mode: A Quantitative Meta-analysis. *Journal of Cognitive Neuroscience*,  
972 21(3), 489–510. <https://doi.org/10.1162/jocn.2008.21029>
- 973 Stolier, R. M., & Freeman, J. B. (2016). Neural pattern similarity reveals the inherent  
974 intersection of social categories. *Nature Neuroscience*, 19(6), 795–797.  
975 <https://doi.org/10.1038/nn.4296>
- 976 Stolier, R. M., & Freeman, J. B. (2017). A Neural Mechanism of Social Categorization.  
977 *The Journal of Neuroscience*, 37(23), 5711–5721.  
978 <https://doi.org/10.1523/JNEUROSCI.3334-16.2017>
- 979 Summerfield, C., Egner, T., Greene, M., Koechlin, E., Mangels, J., & Hirsch, J. (2006).  
980 Predictive Codes for Forthcoming Perception in the Frontal Cortex. *Science*,  
981 314(5803), 1311–1314. <https://doi.org/10.1126/science.1132028>
- 982 Szameitat, A. J., Schubert, T., Müller, K., & Von Yves Cramon, D. (2002). Localization  
983 of executive functions in dual-task performance with fMRI. *Journal of Cognitive*  
984 *Neuroscience*, 14(8), 1184–1199. <https://doi.org/10.1162/089892902760807195>
- 985 Tottenham, N., Tanaka, J. W., Leon, A. C., McCarry, T., Nurse, M., Hare, T. A., &  
986 Nelson, C. (2009). The NimStim set of facial expressions: Judgments from  
987 untrained research participants. *Psychiatry Research*, 168(3), 242–249.  
988 <https://doi.org/http://doi.org/10.1016/j.psychres.2008.05.006>
- 989 Tschentscher, N., Mitchell, D., & Duncan, J. (2017). Fluid Intelligence Predicts Novel  
990 Rule Implementation in a Distributed Frontoparietal Control Network. *The Journal*  
991 *of Neuroscience*, 37(18), 4841–4847. <https://doi.org/10.1523/jneurosci.2478->  
992 16.2017
- 993 Turner, B. (2010). Comparison of methods for the use of pattern classificaion on rapid  
994 event-related fMRI data. In: Annual Meeting of the Society for Neuroscience, San

- 995           Diego, CA.
- 996   van der Wel, P. & van Steenbergen, H. (2018). Pupil dilation as an index of effort in  
997           cognitive control tasks: A review. *Psychonomic Bulletin and Review*, 25, 2005–  
998           2015. <https://doi.org/10.3758/s13423-018-1432-y>
- 999   Waskom, M. L., Kumaran, D., Gordon, A. M., Rissman, J., & Wagner, A. D. (2014).  
1000           Frontoparietal Representations of Task Context Support the Flexible Control of  
1001           Goal-Directed Cognition. *Journal of Neuroscience*, 34(32), 10743–10755.  
1002           <https://doi.org/10.1523/JNEUROSCI.5282-13.2014>
- 1003   Wilson, R. C., Takahashi, Y. K., Schoenbaum, G., & Niv, Y. (2014). Orbitofrontal  
1004           cortex as a cognitive map of task space. *Neuron*, 81(2), 267–279.  
1005           <https://doi.org/10.1016/j.neuron.2013.11.005>
- 1006   Woolgar, A., Hampshire, A., Thompson, R., & Duncan, J. (2011a). Adaptive Coding of  
1007           Task-Relevant Information in Human Frontoparietal Cortex. *Journal of*  
1008           *Neuroscience*, 31(41), 14592–14599. [https://doi.org/10.1523/JNEUROSCI.2616-](https://doi.org/10.1523/JNEUROSCI.2616-11.2011)  
1009           11.2011
- 1010   Woolgar, A., Thompson, R., Bor, D., & Duncan, J. (2011b). Multi-voxel coding of  
1011           stimuli, rules, and responses in human frontoparietal cortex. *NeuroImage*, 56(2),  
1012           744–752. <https://doi.org/10.1016/j.neuroimage.2010.04.035>